CHEMISTRY
A European Journal

Supporting Information

# Mechanistic Insights on Human Phosphoglucomutase Revealed by Transition Path Sampling and Molecular Dynamics Calculations

Natércia F. Brás,*[a, b] Pedro A. Fernandes,[a] Maria J. Ramos,[a] and Steven D. Schwartz[b]

chem_201705090_sm_miscellaneous_information.pdf

# Supporting Information

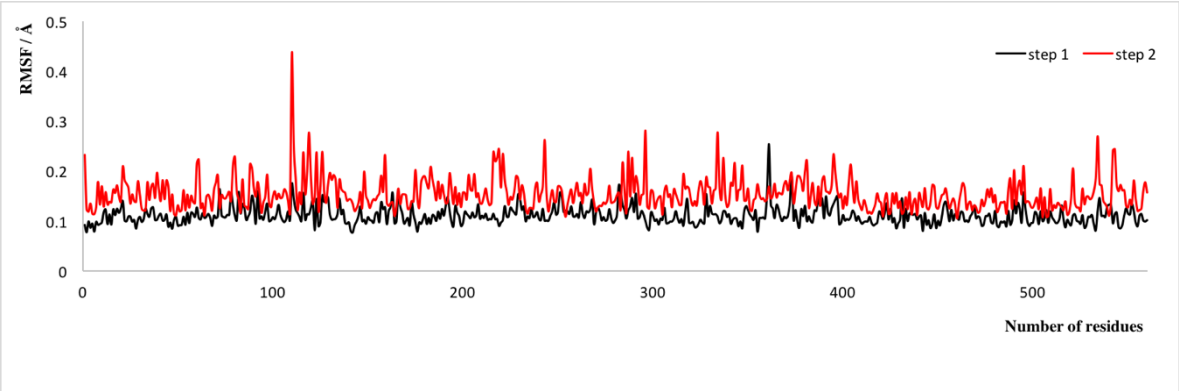


Figure SI-1 – RMSF values obtained for human α-PGM by residue in both mechanistic steps of the catalytic reaction. The values are the average of all reactive trajectories of 500 fs.

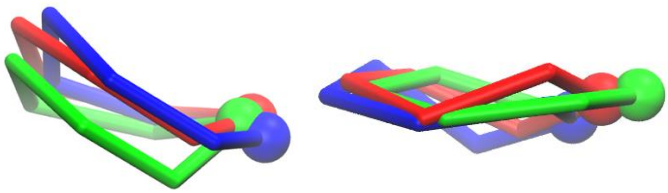

Figure SI-2 – Superimposition of the glucose ring conformations in the three stationary points of the first (left) and second (right) mechanistic step of the human α-PGM reaction. The reactants, TS and products are colored at green, red and blue, respectively. The C1 atom is shown as a sphere.

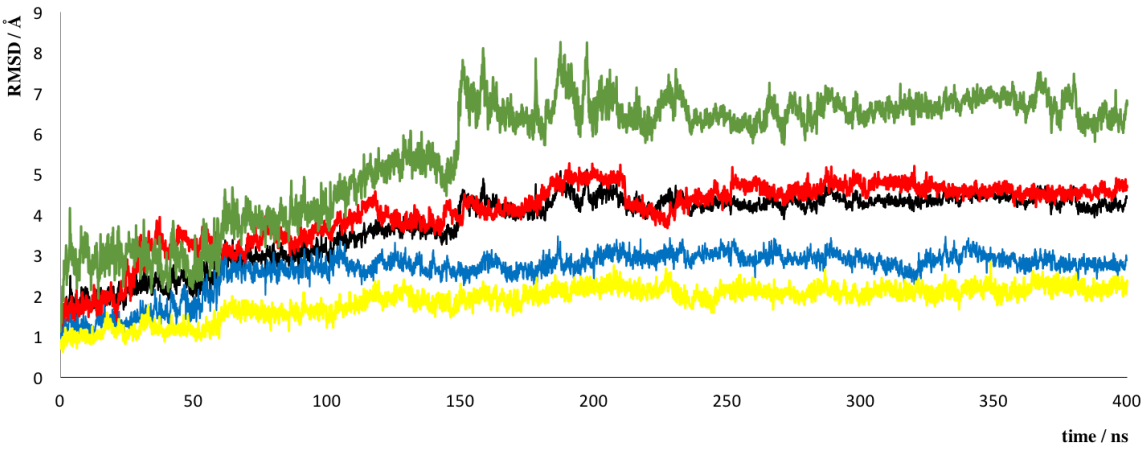


Figure SI-3 – RMSD values obtained for the backbone atoms of entire α-PGM (black line), domain I (blue line), domain II (red line), domain III (yellow line) and domain IV (green line) during simulation A.

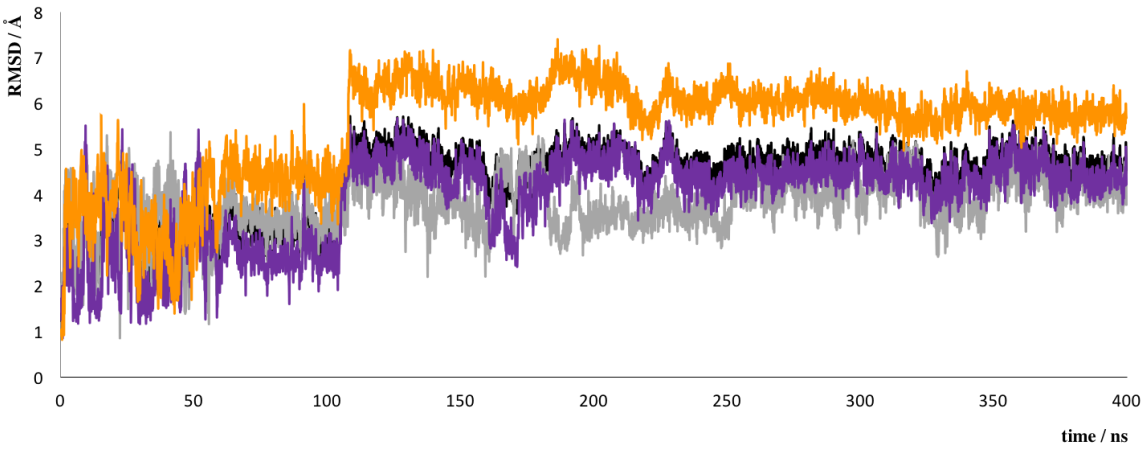


Figure SI-4 – RMSD values obtained for the G16P intermediate (black line), glucose (purple line), P1-$O_3^{2-}$ (gray line) and P6-$O_3^{2-}$ (orange line) groups during simulation A.

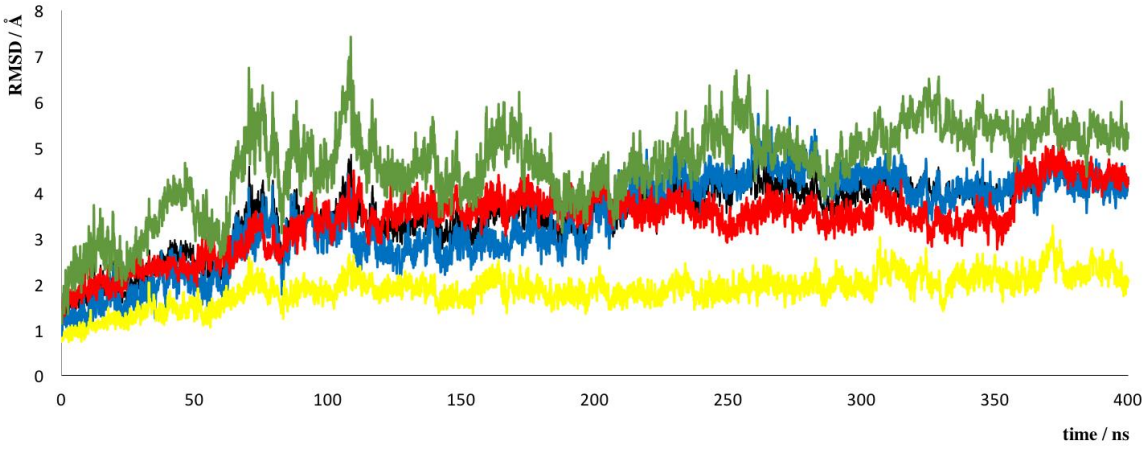


Figure SI-5 – RMSD values obtained for the backbone atoms of entire α-PGM (black line), domain I (blue line), domain II (red line), domain III (yellow line) and domain IV (green line) during simulation B.

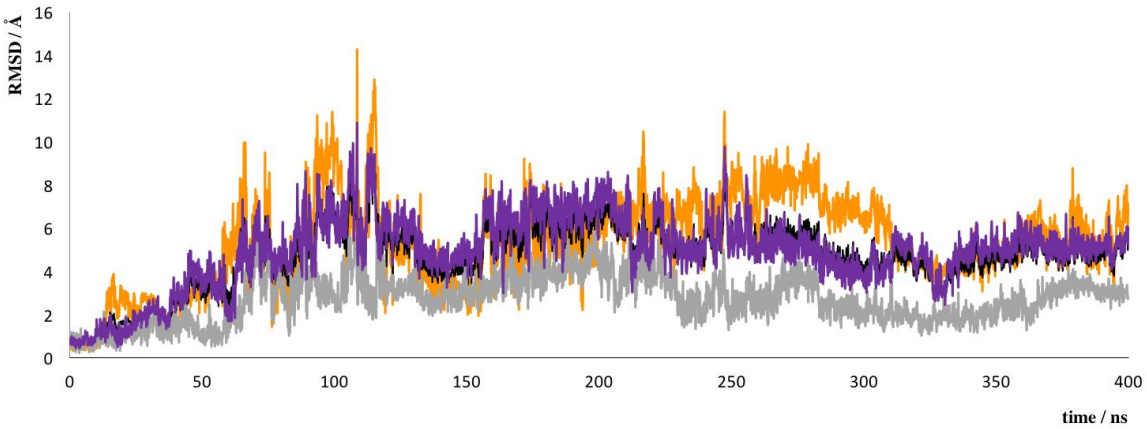

Figure SI-6 – RMSD values obtained for the G16P intermediate (black line), glucose (purple line), P1-$O_3^{2-}$ (gray line) and P6-$O_3^{2-}$ (orange line) groups during simulation B.

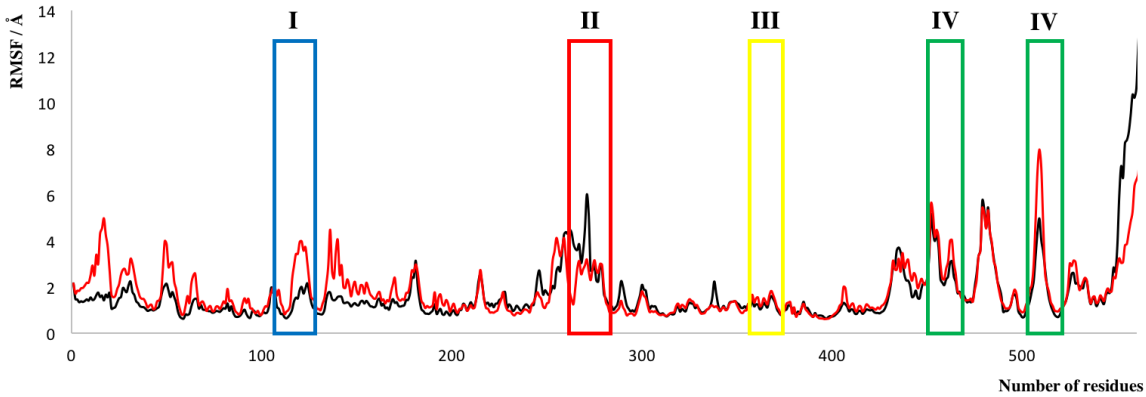


Figure SI-7 – RMSF values obtained for human α-PGM by residue in simulations A (black line) and B (red line). The main loops that belong to the four enzyme domains are also indicated (I – blue, II – red, III – yellow and IV – green).

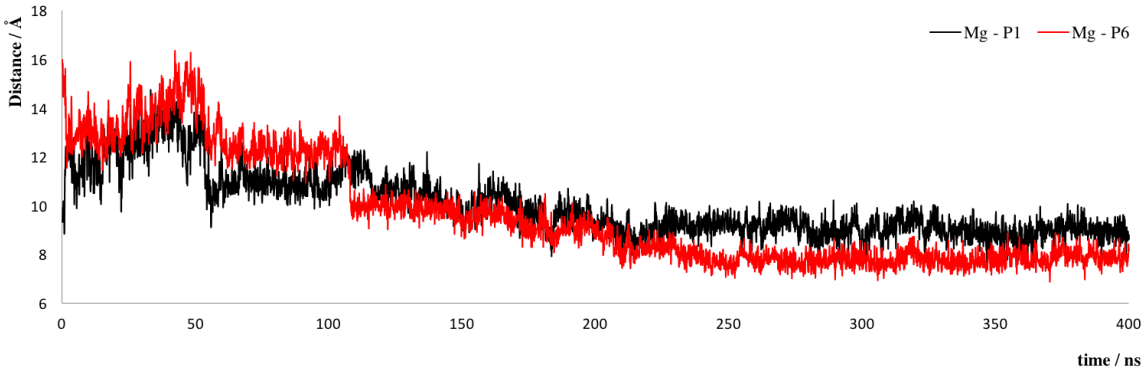


Figure SI-8 – $Mg^{2+}$ – P1 (black line) and $Mg^{2+}$ – P6 (red line) distances throughout simulation A.

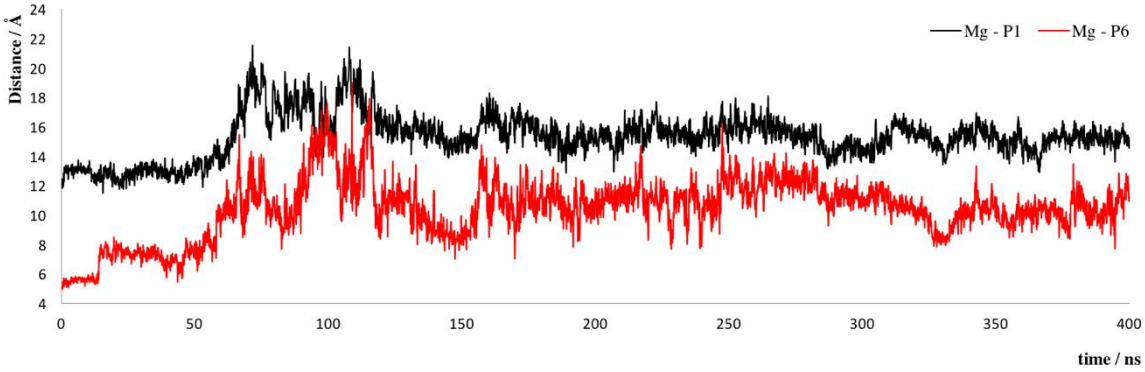


Figure SI-9 – $Mg^{2+}$ – P1 (black line) and $Mg^{2+}$ – P6 (red line) distances throughout simulation B.

*Rearrangements of phosphoryl groups in aMD simulations.* We observed that when the O1-$PO_3^{2-}$ group is near Ser117, its negative charge is stabilized by Arg23. However, after 5 nanoseconds, it reorients to the left-hand side in a concerted way with conformational rearrangements of protein loops I and IV, allowing interactions with Lys130 and the NH backbone groups of Thr19, Ser20, and Gly21. As far as the O6-$PO_3^{2-}$ group is concerned, it is first stabilized by Arg427, Arg503, and Arg515, and during the simulation it reorients to the right-hand side, making an extra interaction with Arg293. This electrostatic effect appears to support and guide the reorientation of the intermediate. Similar conformational alterations were observed for simulation B, with two main differences: the intermediate moves farther away from the active site and the overall protein shows greater motions, which is evidenced by the higher RMSF values obtained for its main loops during this simulation. In this simulation, our time scale (400 ns) was not sufficient to observe the inversion of the $Mg^{2+}$ – P1/P6 distances. This probably happens due to the higher affinity of this specific G16P conformation to interact with the enzymatic binding pocket, or due to the distance of the phosphoryl group to the glucose ring (an extra C-C bond for the O6-$PO_3^{2-}$) that may difficult the rotation of the molecule.

*QM/MM ONIOM calculations.* The same equilibrated α–PGM:G16P structure (previously used as starting geometry for the TPS calculations) was used as starting geometry for the QM/MM ONIOM calculations. Considering the size of the complete TPS model (*ca.* 90,960 atoms), we worked with a reduced model comprising a 5 Å radius sphere of water molecules cut around the protein:substrate system. The final system was composed by 12,787 atoms. The system was divided into two layers, within the ONIOM formalism[1] as implemented in Gaussian 09 software[2]. The high-level layer is those used in the previous TPS calculations. The high-layer was described with density functional theory (DFT) at the unrestricted B3LYP/6-31G(d) level of theory for geometry optimizations, which was shown to provide accurate results in previous enzymatic mechanistic studies[3]. The remaining atoms of the system were treated at the molecular mechanics (MM) level with the ff99SB. Hydrogen atoms were used as link atoms. The mechanical embedding scheme was used to describe the Coulomb interaction between the two layers. The van der Waals QM-MM interactions were treated with classical potentials.

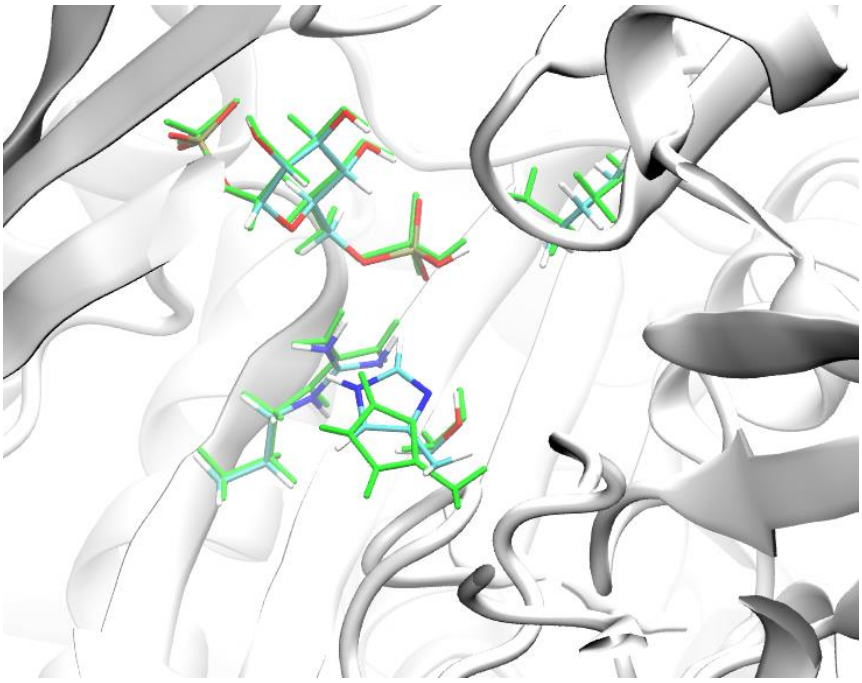

Figure SI-10 – Superimposition of the reactant state geometries of the first mechanistic step of the human α-PGM reaction optimized with DFT and PM3 methods. The QM region optimized with DFT and PM3 approaches are colored at element type and green, respectively.

Table SI-1 – Lengths of the key breaking-bonds and forming-bonds along the reactants, TS and products for the G16P to G1P step. All values are in angstrom.

| state | reactive trajectory | O-Ser117 – P6 | O6 – P6 | Nδ-His118 – HO-Ser117 | HZ3-Lys389 – O6 | O-Ser117 – $Mg^{2+}$ | O-$PO_3^{2-}$ – $Mg^{2+}$ | O-$PO_3^{2-}$ – $H_2N$-Arg23 |
|---|---|---|---|---|---|---|---|---|
| reactants | 1 | 3.46 | 1.61 | 2.93 | 1.97 | 2.41 | 1.78 | 3.59 |
| | 2 | 3.09 | 1.68 | 2.77 | 2.97 | 2.75 | 1.72 | 3.86 |
| | 3 | 3.44 | 1.99 | 3.30 | 0.88 | 2.03 | 1.88 | 4.54 |
| | 4 | 3.63 | 2.26 | 4.21 | 1.09 | 3.44 | 1.79 | 4.43 |
| | 5 | 3.76 | 2.42 | 3.44 | 0.94 | 2.22 | 1.77 | 5.12 |
| | 6 | 3.67 | 1.75 | 2.91 | 3.77 | 3.02 | 1.73 | 3.82 |

| | | | | | | | | |
|---|---|---|---|---|---|---|---|---|
| | 7 | 3.57 | 1.71 | 2.18 | 3.15 | 2.97 | 1.74 | 3.88 |
| | 8 | 3.50 | 1.64 | 2.98 | 3.38 | 2.90 | 1.76 | 3.93 |
| | 9 | 4.14 | 2.50 | 3.40 | 1.11 | 2.24 | 1.96 | 3.83 |
| | 10 | 3.80 | 1.76 | 3.64 | 3.41 | 1.83 | 2.08 | 5.11 |
| | 11 | 3.53 | 2.07 | 3.48 | 1.00 | 2.08 | 1.85 | 4.78 |
| | 12 | 4.07 | 2.32 | 5.59 | 0.91 | 2.03 | 1.72 | 4.73 |
| | *average* | 3.64 | 1.98 | 3.40 | 2.05 | 2.49 | 1.82 | 4.30 |
| | *SD* | 0.28 | 0.33 | 0.86 | 1.19 | 0.51 | 0.11 | 0.55 |
| | 1 | 2.41 | 2.92 | 0.99 | 0.86 | 2.80 | 1.82 | 3.75 |
| | 2 | 2.42 | 2.88 | 1.01 | 0.84 | 2.86 | 1.88 | 3.90 |
| | 3 | 2.54 | 2.98 | 1.07 | 0.90 | 2.88 | 1.72 | 3.93 |
| | 4 | 2.67 | 3.17 | 1.02 | 1.13 | 3.04 | 1.74 | 3.51 |
| | 5 | 2.73 | 3.39 | 1.02 | 0.93 | 3.01 | 1.71 | 3.33 |
| | 6 | 2.45 | 2.97 | 0.94 | 1.06 | 2.77 | 1.74 | 3.65 |
| | 7 | 2.57 | 2.88 | 0.95 | 1.06 | 2.93 | 1.83 | 3.99 |
| | 8 | 2.57 | 2.88 | 0.94 | 1.02 | 2.91 | 1.83 | 3.99 |
| | 9 | 2.67 | 3.40 | 0.99 | 1.15 | 3.04 | 1.78 | 3.54 |
| | 10 | 2.64 | 3.37 | 1.06 | 0.88 | 3.01 | 0.68 | 4.30 |
| | 11 | 2.46 | 2.80 | 1.10 | 0.95 | 3.03 | 1.92 | 3.89 |
| | 12 | 2.40 | 3.14 | 1.04 | 1.02 | 2.86 | 1.68 | 3.67 |
| | *average* | 2.54 | 3.07 | 1.01 | 0.98 | 2.93 | 1.69 | 3.79 |
| **TS** | *SD* | 0.12 | 0.22 | 0.05 | 0.10 | 0.10 | 0.33 | 0.26 |
| | 1 | 1.88 | 3.74 | 0.94 | 1.14 | 2.23 | 1.73 | 1.93 |
| | 2 | 1.80 | 3.45 | 1.01 | 1.02 | 2.08 | 1.77 | 1.94 |
| | 3 | 1.74 | 3.63 | 1.14 | 1.04 | 1.91 | 1.77 | 2.28 |
| | 4 | 1.78 | 3.55 | 1.02 | 1.12 | 2.51 | 1.74 | 1.83 |
| | 5 | 1.72 | 3.11 | 1.04 | 1.14 | 2.49 | 1.73 | 1.60 |
| | 6 | 1.89 | 3.73 | 0.96 | 0.92 | 2.40 | 1.75 | 1.47 |
| | 7 | 1.81 | 3.78 | 1.02 | 0.96 | 2.15 | 1.74 | 1.59 |
| | 8 | 1.79 | 3.81 | 1.08 | 1.06 | 2.19 | 1.74 | 1.57 |
| | 9 | 1.89 | 3.49 | 1.06 | 0.99 | 2.07 | 1.75 | 1.56 |
| | 10 | 1.87 | 3.09 | 1.02 | 0.97 | 2.11 | 1.72 | 2.25 |
| | 11 | 1.86 | 3.12 | 1.02 | 0.90 | 2.13 | 1.77 | 1.83 |
| | 12 | 1.80 | 3.75 | 1.07 | 1.03 | 2.04 | 1.76 | 1.86 |
| | *average* | 1.82 | 3.52 | 1.03 | 1.02 | 2.19 | 1.75 | 1.81 |
| **products** | *SD* | 0.06 | 0.27 | 0.05 | 0.08 | 0.19 | 0.02 | 0.27 |

Table SI-2 – Lengths of the key breaking-bonds and forming-bonds along the reactants, TS and products for the G16P to G1P step. All values are in angstrom.

| state | reactive trajectory | O-Ser117 – P1 | O1 – P1 | Nδ-His118 – HO-Ser117 | HZ3-Lys389 – O1 | O-Ser117 – $Mg^{2+}$ | O-$PO_3^{2-}$ – $Mg^{2+}$ | O-$PO_3^{2-}$ – $H_2N$-Arg23 |
|---|---|---|---|---|---|---|---|---|
| | 1 | 3.75 | 1.86 | 3.86 | 3.64 | 2.34 | 1.68 | 5.34 |
| | 2 | 3.54 | 2.00 | 3.86 | 3.02 | 2.58 | 1.71 | 3.47 |
| | 3 | 2.80 | 1.74 | 2.31 | 2.44 | 3.25 | 1.74 | 3.43 |
| | 4 | 3.71 | 1.82 | 4.34 | 4.08 | 1.89 | 2.00 | 3.57 |
| | 5 | 2.77 | 2.00 | 3.65 | 2.30 | 3.31 | 1.84 | 3.77 |
| | 6 | 4.02 | 1.87 | 3.22 | 4.58 | 2.69 | 2.00 | 3.81 |
| | 7 | 3.33 | 1.75 | 3.48 | 3.75 | 3.38 | 1.96 | 3.74 |
| | 8 | 3.75 | 1.86 | 3.86 | 3.57 | 2.46 | 2.04 | 3.79 |
| | 9 | 3.32 | 1.89 | 3.05 | 3.07 | 2.97 | 1.92 | 3.13 |
| | 10 | 3.50 | 1.75 | 3.69 | 3.55 | 3.14 | 1.84 | 4.07 |
| | 11 | 2.97 | 1.80 | 3.83 | 3.42 | 1.95 | 1.82 | 2.91 |
| | 12 | 3.88 | 1.73 | 5.55 | 3.38 | 1.91 | 2.64 | 2.97 |
| | *average* | 3.45 | 1.84 | 3.73 | 3.40 | 2.66 | 1.93 | 3.67 |
| **reactants** | *SD* | 0.42 | 0.09 | 0.77 | 0.64 | 0.56 | 0.25 | 0.64 |
| | 1 | 2.80 | 3.67 | 1.27 | 1.03 | 3.92 | 1.73 | 3.26 |
| | 2 | 2.66 | 3.48 | 1.38 | 1.16 | 3.75 | 1.72 | 3.37 |
| | 3 | 2.46 | 3.04 | 1.29 | 1.14 | 3.30 | 1.68 | 3.43 |
| | 4 | 2.42 | 3.04 | 1.23 | 1.57 | 3.34 | 1.65 | 3.54 |
| | 5 | 2.30 | 2.97 | 1.12 | 1.24 | 3.16 | 1.63 | 3.53 |
| | 6 | 2.44 | 3.00 | 1.31 | 0.97 | 3.26 | 1.66 | 3.43 |
| | 7 | 2.50 | 3.20 | 1.40 | 1.23 | 3.27 | 1.78 | 3.51 |
| | 8 | 2.48 | 3.33 | 1.31 | 1.25 | 3.55 | 1.80 | 3.33 |
| | 9 | 2.00 | 2.96 | 1.38 | 1.13 | 3.14 | 1.66 | 3.71 |
| | 10 | 2.52 | 3.35 | 0.95 | 1.06 | 3.12 | 1.80 | 3.64 |
| | 11 | 2.79 | 3.31 | 1.02 | 1.12 | 2.80 | 1.78 | 3.92 |
| | 12 | 2.06 | 3.17 | 1.29 | 1.90 | 2.89 | 1.74 | 3.57 |
| | *average* | 2.45 | 3.21 | 1.25 | 1.23 | 3.29 | 1.72 | 3.52 |
| **TS** | *SD* | 0.25 | 0.22 | 0.14 | 0.26 | 0.32 | 0.06 | 0.18 |
| | 1 | 2.13 | 5.30 | 1.12 | 1.06 | 1.98 | 1.89 | 2.78 |
| | 2 | 1.83 | 4.43 | 0.89 | 1.13 | 2.19 | 1.76 | 2.32 |
| **products** | 3 | 1.95 | 3.44 | 0.99 | 0.98 | 1.97 | 1.93 | 3.41 |

| | | | | | | | | |
|---|---|---|---|---|---|---|---|---|
| | 4 | 1.96 | 4.90 | 0.90 | 1.04 | 2.92 | 1.73 | 3.33 |
| | 5 | 2.00 | 3.56 | 1.00 | 0.95 | 2.11 | 1.84 | 3.55 |
| | 6 | 1.71 | 2.72 | 1.11 | 0.98 | 2.99 | 1.69 | 3.33 |
| | 7 | 1.89 | 4.27 | 0.85 | 1.02 | 1.95 | 1.80 | 3.22 |
| | 8 | 1.69 | 3.26 | 0.94 | 1.01 | 2.59 | 1.76 | 2.57 |
| | 9 | 1.80 | 3.66 | 1.11 | 0.95 | 2.48 | 1.76 | 3.78 |
| | 10 | 2.28 | 4.31 | 0.90 | 0.90 | 2.15 | 1.88 | 3.16 |
| | 11 | 1.94 | 4.70 | 0.88 | 0.84 | 2.61 | 1.80 | 1.95 |
| | 12 | 2.30 | 4.65 | 0.89 | 0.93 | 2.90 | 1.81 | 4.03 |
| | *average* | 1.96 | 4.10 | 0.97 | 0.98 | 2.40 | 1.80 | 3.12 |
| | *SD* | 0.20 | 0.77 | 0.10 | 0.08 | 0.39 | 0.07 | 0.61 |


[1] F. Maseras and K. Morokuma, *Journal of Computational Chemistry* **1995**, *16*, 1170-1179.

[2] Frisch, M. J.; Trucks, G. W.; Schlegel, H. B.; Scuseria, G. E.; Robb, M. A.; Cheeseman, J. R.; Scalmani, G.; Barone, V.; Mennucci, B.; Petersson, G. A.; Nakatsuji, H.; Caricato, M.; Li, X.; Hratchian, H. P.; Izmaylov, A. F.; Bloino, J.; Zheng, G.; Sonnenberg, J. L.; Hada, M.; Ehara, M.; Toyota, K.; Fukuda, R.; Hasegawa, J.; Ishida, M.; Nakajima, T.; Honda, Y.; Kitao, O.; Nakai, H.; Vreven, T.; Montgomery, Jr., J. A.; Peralta, J. E.; Ogliaro, F.; Bearpark, M.; Heyd, J. J.; Brothers, E.; Kudin, K. N.; Staroverov, V. N.; Kobayashi, R.; Normand, J.; Raghavachari, K.; Rendell, A.; Burant, J. C.; Iyengar, S. S.; Tomasi, J.; Cossi, M.; Rega, N.; Millam, N. J.; Klene, M.; Knox, J. E.; Cross, J. B.; Bakken, V.; Adamo, C.; Jaramillo, J.; Gomperts, R.; Stratmann, R. E.; Yazyev, O.; Austin, A. J.; Cammi, R.; Pomelli, C.; Ochterski, J. W.; Martin, R. L.; Morokuma, K.; Zakrzewski, V. G.; Voth, G. A.; Salvador, P.; Dannenberg, J. J.; Dapprich, S.; Daniels, A. D.; Farkas, Ö.; Foresman, J. B.; Ortiz, J. V.; Cioslowski, J.; Fox, D. J. in *Gaussian 09*, *Vol.* Gaussian, Inc., Wallingford CT, **2009**.

[3] a) N. F. Bras, P. A. Fernandes and M. J. Ramos, *ACS Catalysis* **2014**, *4*, 2587-2597; b) N. F. Bras, P. Ferreira, A. R. Calixto, M. Jaspars, W. Houssen, J. H. Naismith, P. A. Fernandes and M. J. Ramos, *Chemistry* **2016**, *22*, 13089-13097; c) R. P. Sousa, P. A. Fernandes, M. J. Ramos and N. F. Bras, *Phys Chem Chem Phys* **2016**, *18*, 11488-11496.